

Supporting Information:

Biogeochemical Impact of Cable Bacteria in Coastal Black Sea Sediment

Martijn Hermans,^{1,2} Nils Risgaard-Petersen,^{3,4} Filip J.R. Meysman,^{5,6} and Caroline P. Slomp¹

¹Department of Earth Sciences, Faculty of Geosciences, Utrecht University, 3584 CB Utrecht, the Netherlands

²Now at: Aquatic Biogeochemistry Research Unit (ABRU), Ecosystems and Environment Research Programme, Faculty of Biological and Environmental Sciences, University of Helsinki, 00790 Helsinki, Finland

³Center for Geomicrobiology, Section for Microbiology, Department of Bioscience, Aarhus University, 8000 Aarhus, Denmark

⁴Center for Electromicrobiology, Section for Microbiology, Department of Bioscience, Aarhus University, 8000 Aarhus, Denmark

⁵Center of Excellence for Microbial Systems Technology, Department of Biology, University of Antwerp, 2610 Wilrijk, Belgium

⁶Department of Biotechnology, Delft University of Technology, 2629 HZ Delft, the Netherlands

S1.1. Porosity

Table S1. Depth profile of the porosity calculated from the water loss upon freeze-drying and sediment density following Burdige (2006) for one core.

Depth [cm]			Porosity [vol vol ⁻¹]
0	-	0.5	0.90
0.5	-	1	0.89
1	-	1.5	0.89
1.5	-	2	0.90
2	-	2.5	0.84
2.5	-	3	0.84
3	-	3.5	0.81
3.5	-	4	0.81
4	-	4.5	0.81
4.5	-	5	0.81

S1.2. Sequential Extractions

Table S2. Sequential extraction scheme for Fe, S and P.

Extracted mineral phase	Solvent	Time
Sequential Fe extraction^{1,2}		
1 Labile ferric Fe oxides (ferrihydrite, akaganéite and lepidocrocite) ferrous Fe (FeS and FeCO ₃) ¹	1 M HCl	4 h
2 Crystalline Fe oxides ¹	0.35 M acetic acid / 0.2 M sodium citrate with 50 g L ⁻¹ sodium dithionite, pH 4.8	4 h
3 Magnetite ²	0.2 M / 0.14 M	6 h
4 Pyrite ¹	HNO ₃ (65-70%)	2 h
Sequential S extraction^{3,4}		
1 Acid volatile sulphur (AVS)	6 M HCl	24 h
2 Elemental sulphur (S ₀)	Methanol (99.8%)	16 h
3 Chromium reducible sulfur (CRS)	500 g/L chromous chloride in 32% HCl	48 h
Sequential P extraction⁵		
1 Exchangeable P	1 M MgCl ₂ to pH 8	30 min
2 Easily reducible or reactive ferric Fe-bound P (CDB-P)	Citrate-bicarbonate-CDB buffered to pH 7.5 with sodium citrate / sodium bicarbonate	8 h
	1 M MgCl ₂ to pH 8 (wash step)	30 min
3 Authigenic P	1 M sodium acetate buffered to pH 4 with acetic acid	6 h
	1 M MgCl ₂ to pH 8 (wash step)	30 min
4 Detrital P	1 M HCl	24 h
5 Organic P	1 M HCl, after ashing at 550 °C	24 h

¹ Claff et al. (2010)

² Poulton and Canfield (2005)

³ Burton et al. (2006)

⁴ Burton et al. (2008)

⁵ Ruttenberg (1992) as modified by Slomp et al. (1996)

S1.3. FISH Image of Filamentous Cable Bacteria

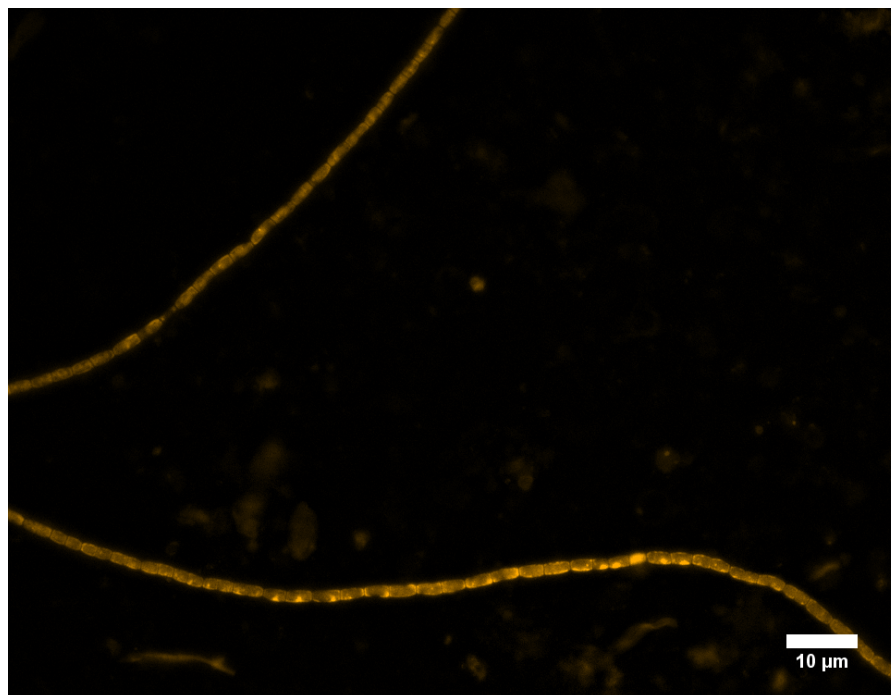


Figure S1. Microscopic FISH image of two cable bacteria filaments. These filaments were extracted from the surface sediment 207 days after the start of the incubation experiment. The white scale bar denotes a distance of 10 μm .

S1.4. Time-series of Oxygen Penetration Depth

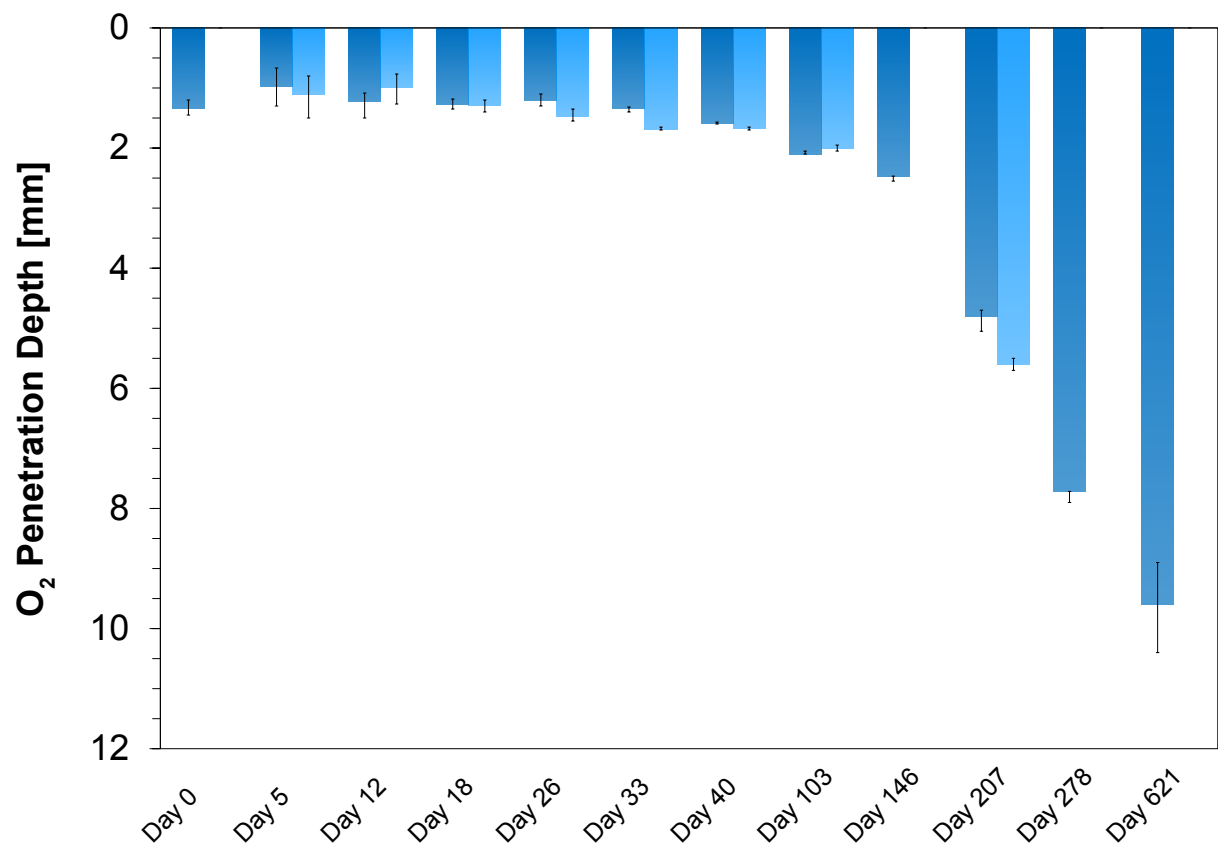


Figure S2. Time-series of the O₂ penetration depth in the surface sediment in mm in two sediment cores. These O₂ penetration depths represent the average value of 3 replicate measurements per core. The error bars represent the minimum and maximum O₂ penetration depths.

S1.5. Anoxic Control Core

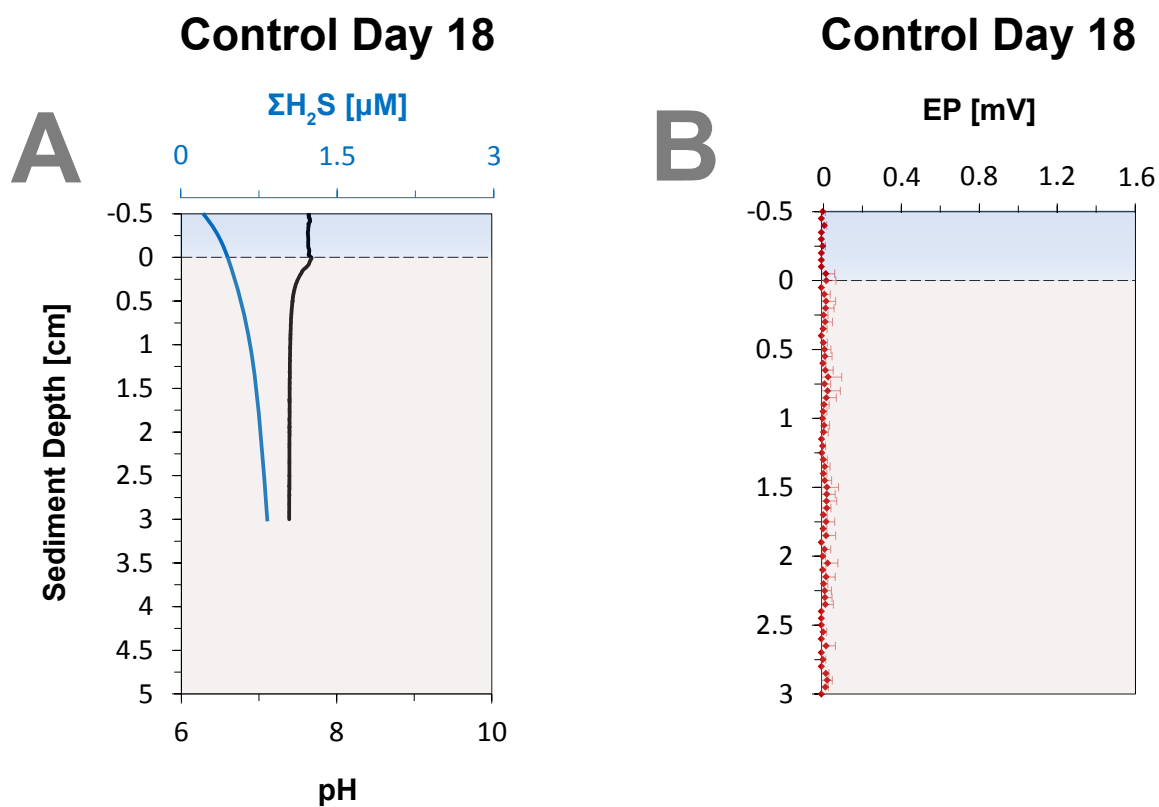


Figure S3. pH and $\Sigma\text{H}_2\text{S}$ and EP for the anoxic control core at day 18. The pore water depth profiles for the other time points look similar.

S1.6. Linear Pore Water Gradients of NH_4^+ , SO_4^{2-} , Fe^{2+} , Mn^{2+} , Ca^{2+} and H_4SiO_4 used for Diffusive Fluxes

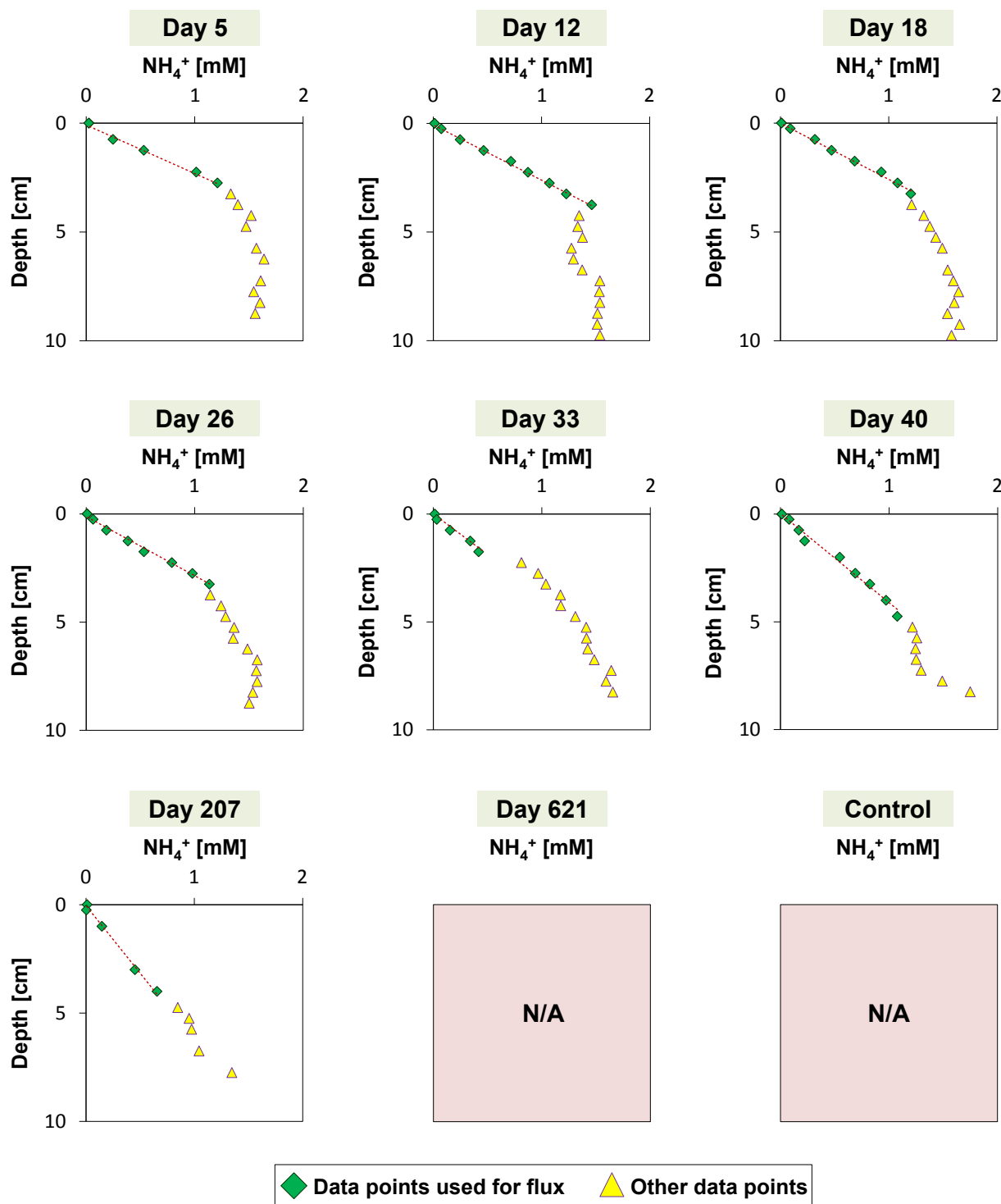


Figure S4. Time-series of pore water depth profiles of NH_4^+ . The linear gradient in the green and cyan diamonds represents data points that were used for the calculation of the upward NH_4^+ flux, whereas the yellow and pink triangles are data points that were not used for this calculation.

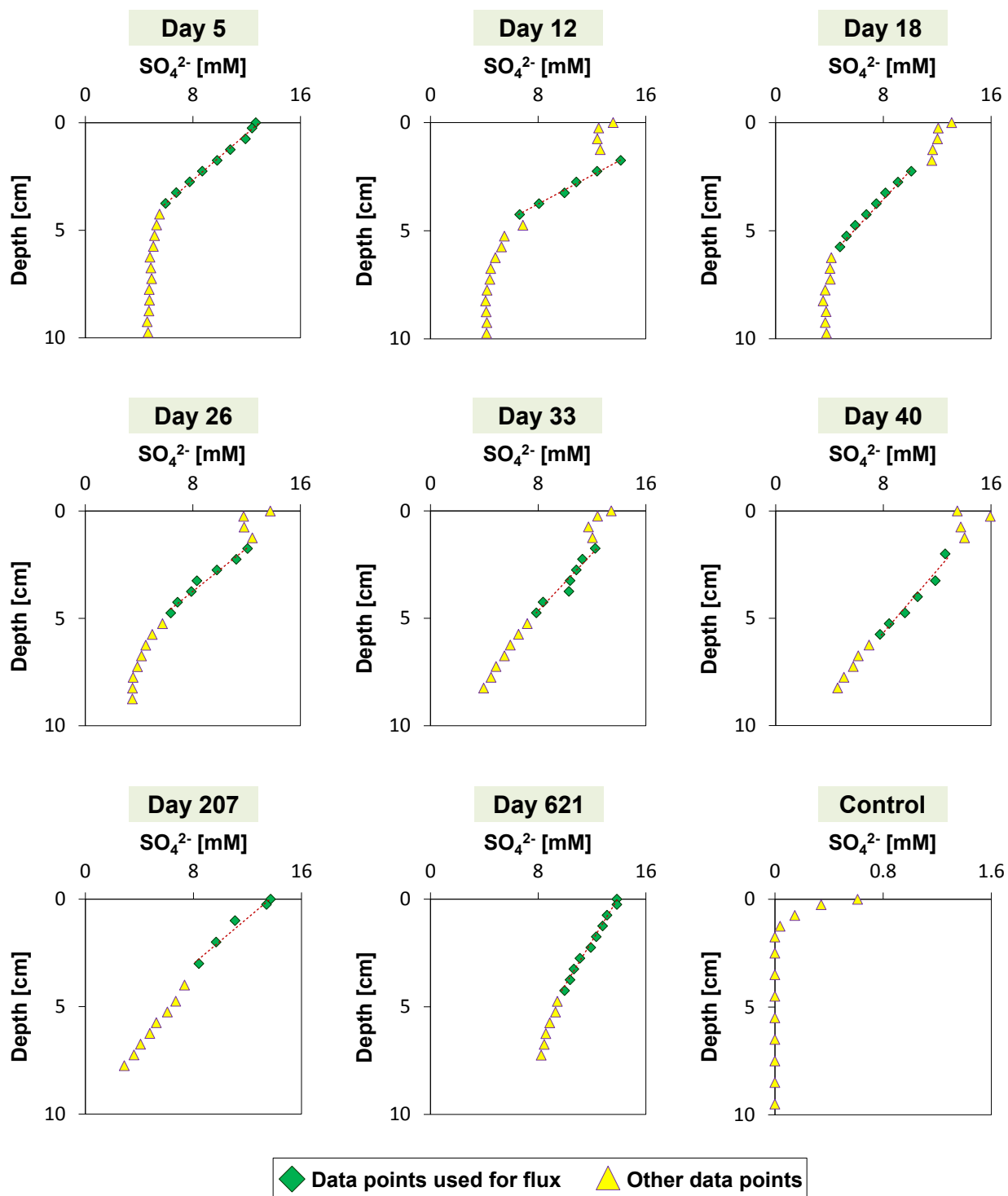


Figure S5. Time-series of pore water depth profiles of SO_4^{2-} . The linear gradient in the green diamonds represents data points that were used for the calculation of the downward SO_4^{2-} flux, whereas the yellow triangles are data points that were not used for this calculation.

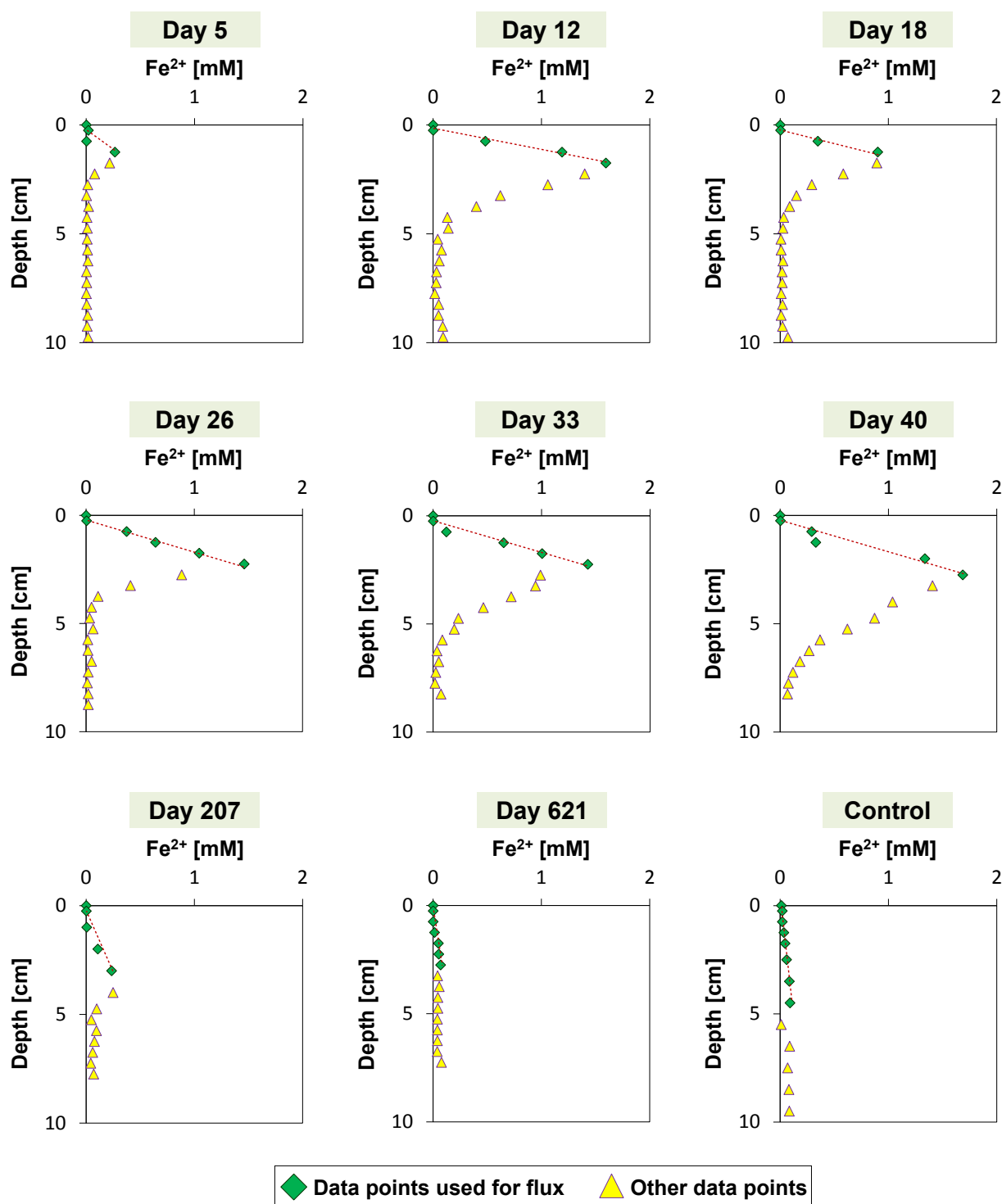


Figure S6. Time-series of pore water depth profiles of dissolved Fe^{2+} . The linear gradient in the green diamonds represents data points that were used for the calculation of the upward Fe^{2+} flux, whereas the yellow triangles are data points that were not used for this calculation.

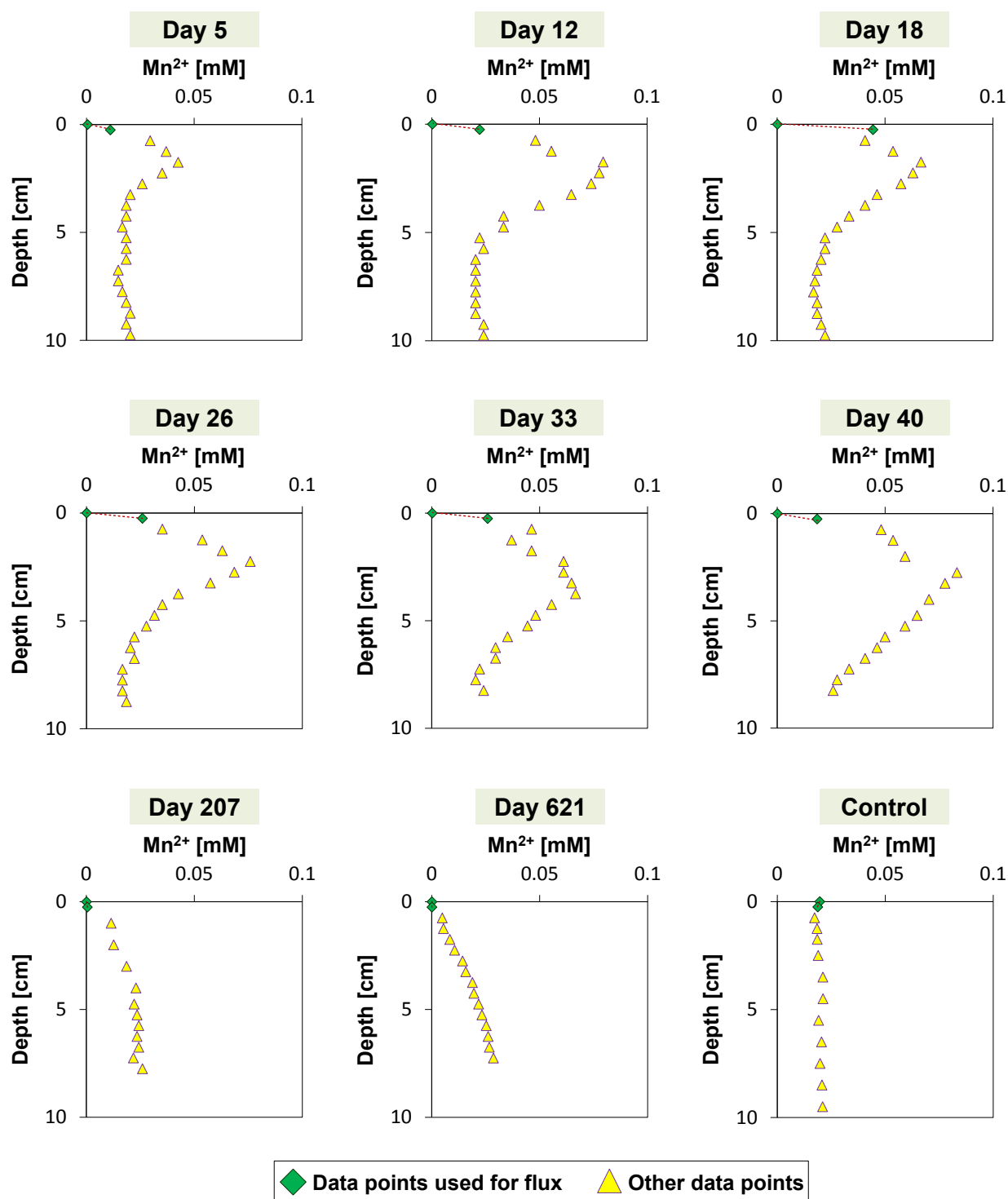


Figure S7. Time-series of pore water depth profiles of dissolved Mn^{2+} . The linear gradient in the green diamonds represents data points that were used for the calculation of the upward Mn^{2+} flux, whereas the yellow triangles are data points that were not used for this calculation.

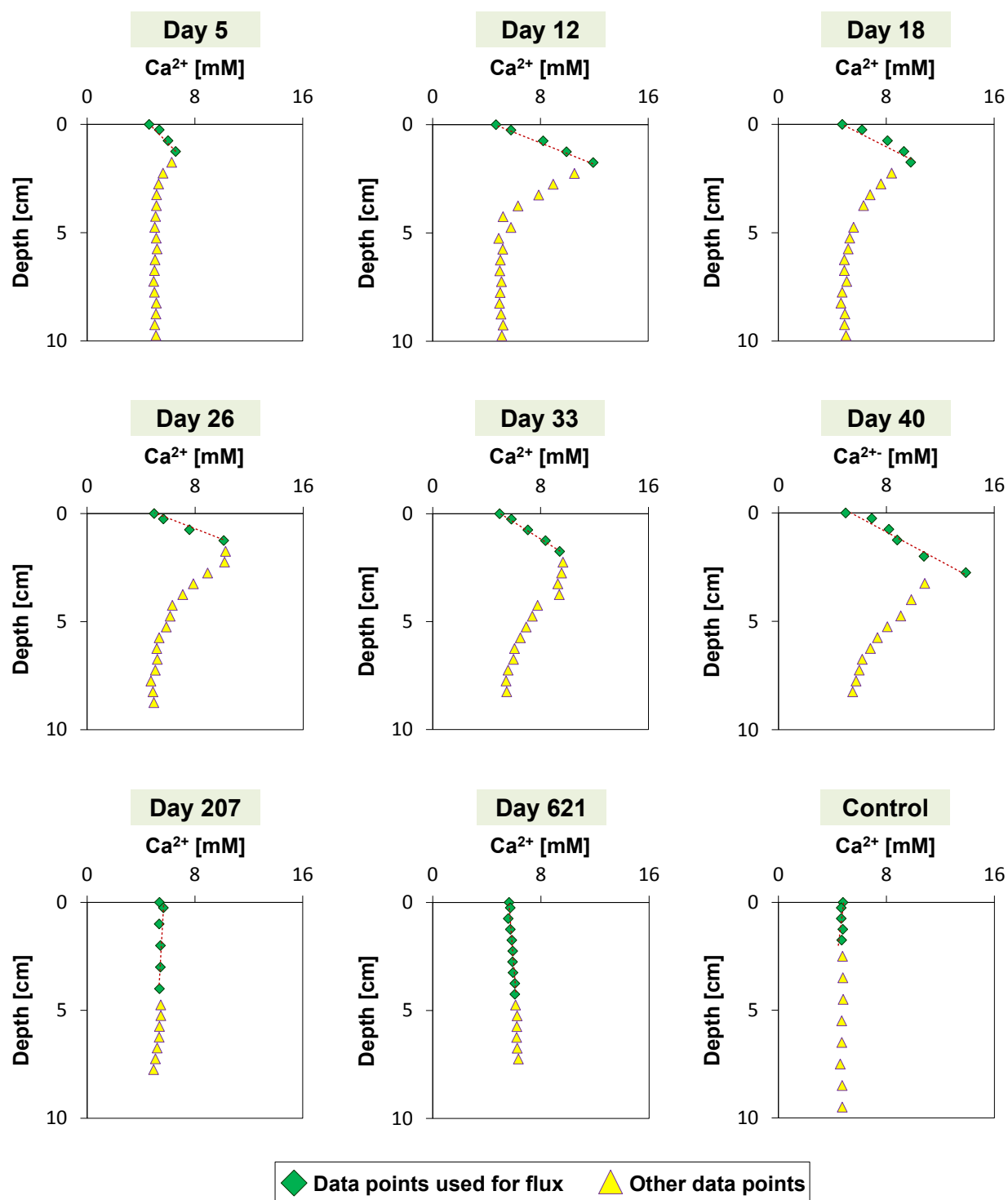


Figure S8. Time-series of pore water depth profiles of dissolved Ca^{2+} . The linear gradient in the green diamonds represents data points that were used for the calculation of the upward Ca^{2+} flux, whereas the yellow triangles are data points that were not used for this calculation.

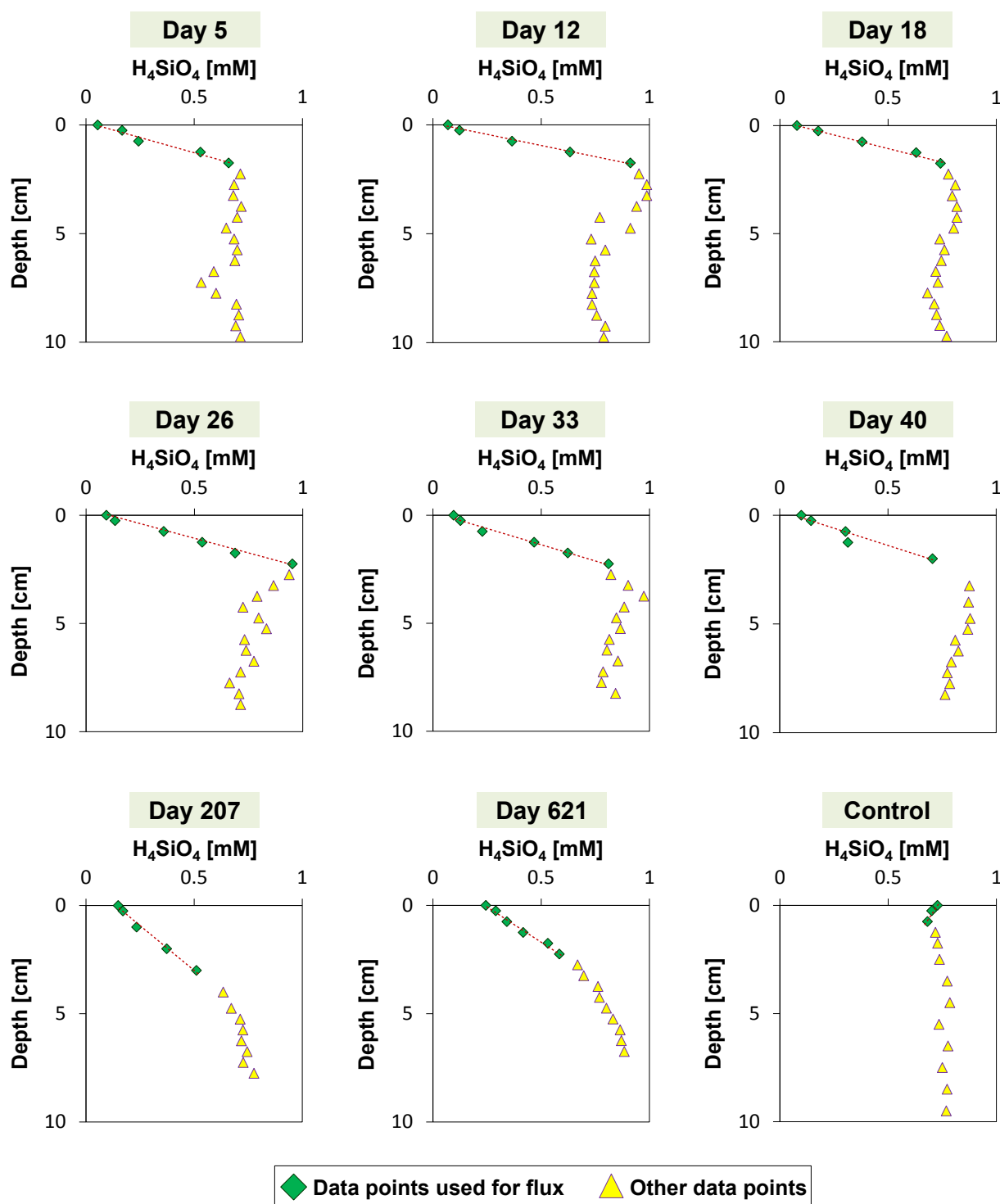


Figure S9. Time-series of pore water depth profiles of dissolved H_4SiO_4 . The linear gradient in the green diamonds represents data points that were used for the calculation of the upward H_4SiO_4 flux, whereas the yellow triangles are data points that were not used for this calculation.

Table S3. Diffusive fluxes of NH_4^+ , SO_4^{2-} , Fe^{2+} , Mn^{2+} , Ca^{2+} and H_4SiO_4 in $\text{mmol m}^{-2} \text{d}^{-1}$. Positive values indicate an upward flux, whereas negative values represent a downward flux.

	NH_4^+ ($\text{mmol m}^{-2} \text{d}^{-1}$)	SO_4^{2-} ($\text{mmol m}^{-2} \text{d}^{-1}$)	Fe^{2+} ($\text{mmol m}^{-2} \text{d}^{-1}$)	Mn^{2+} ($\text{mmol m}^{-2} \text{d}^{-1}$)	Ca^{2+} ($\text{mmol m}^{-2} \text{d}^{-1}$)	H_4SiO_4 ($\text{mmol m}^{-2} \text{d}^{-1}$)
Day 5	4.71	-10.49	0.82	0.16	6.95	2.01
Day 12	4.23	-17.60	3.54	0.34	18.23	2.80
Day 18	4.02	-8.87	2.80	0.68	12.83	2.20
Day 26	3.79	-11.15	2.52	0.40	18.20	2.22
Day 33	2.53	-8.54	2.46	0.40	11.25	1.85
Day 40	2.44	-7.57	2.38	0.28	14.33	1.76
Day 207	1.76	-10.38	0.32	0.01	0.00	0.70
Day 621	N/A	-5.36	0.10	0.00	0.45	0.88
Control (Day 621)	N/A	N/A	0.07	0.00	-0.23	-0.36

S1.7. Solute Fluxes

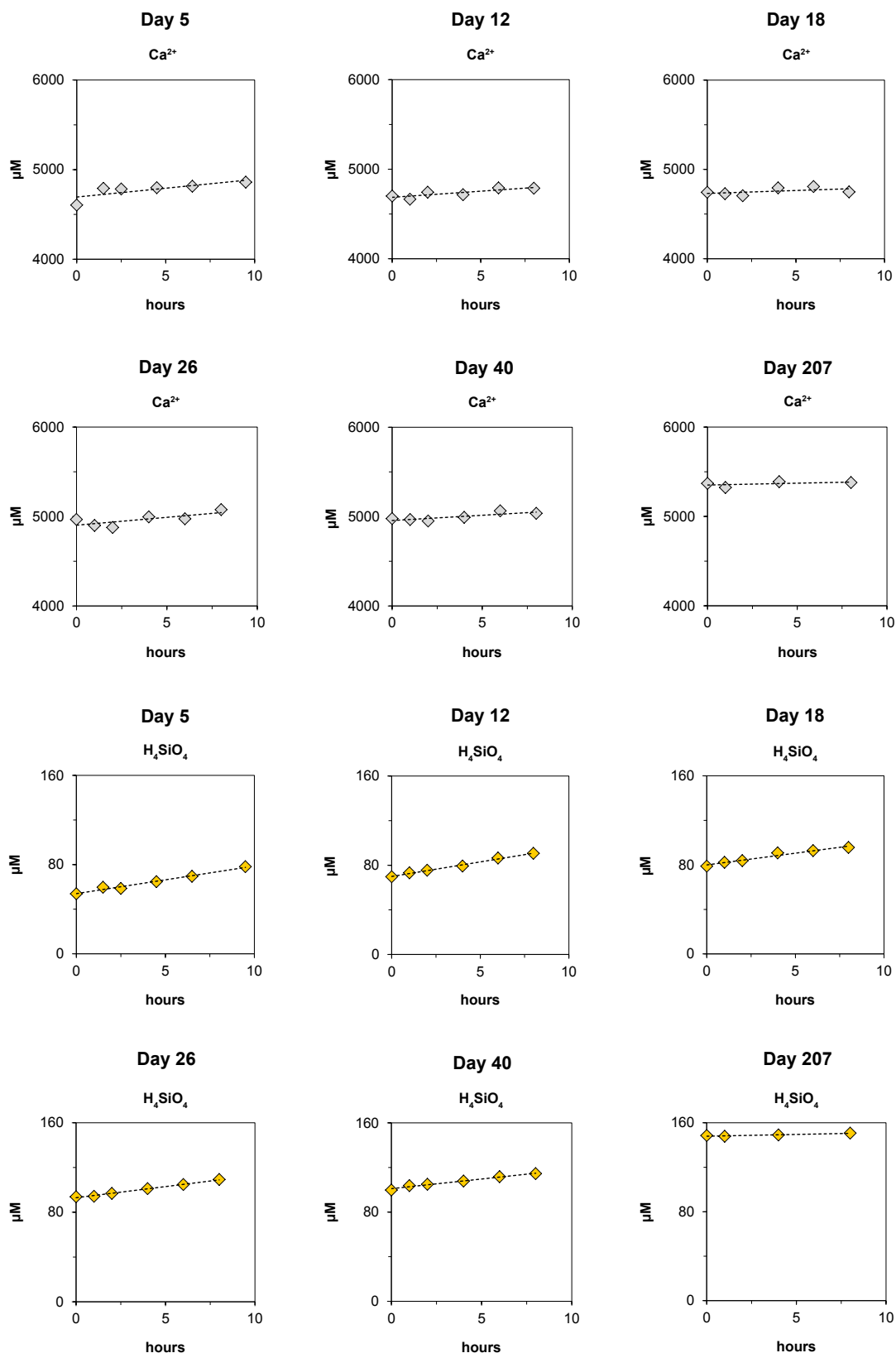


Figure S10. Concentrations of Ca^{2+} and H_4SiO_4 in the overlying water during solute flux incubations over an 8 hour time period for day 5, 12, 18, 26, 40 and 207. The linear gradient was used for the calculation of the fluxes.

Table S4. Solute fluxes of Ca^{2+} and H_4SiO_4 in $\text{mmol m}^{-2} \text{d}^{-1}$.

	Ca^{2+} ($\text{mmol m}^{-2} \text{d}^{-1}$)	H_4SiO_4 ($\text{mmol m}^{-2} \text{d}^{-1}$)
Day 5	19.38	1.84
Day 12	7.88	1.89
Day 18	0.46	1.51
Day 26	9.95	1.39
Day 40	5.27	1.33
Day 207	0.88	0.20

S1.8. Time-series of Core Photographs

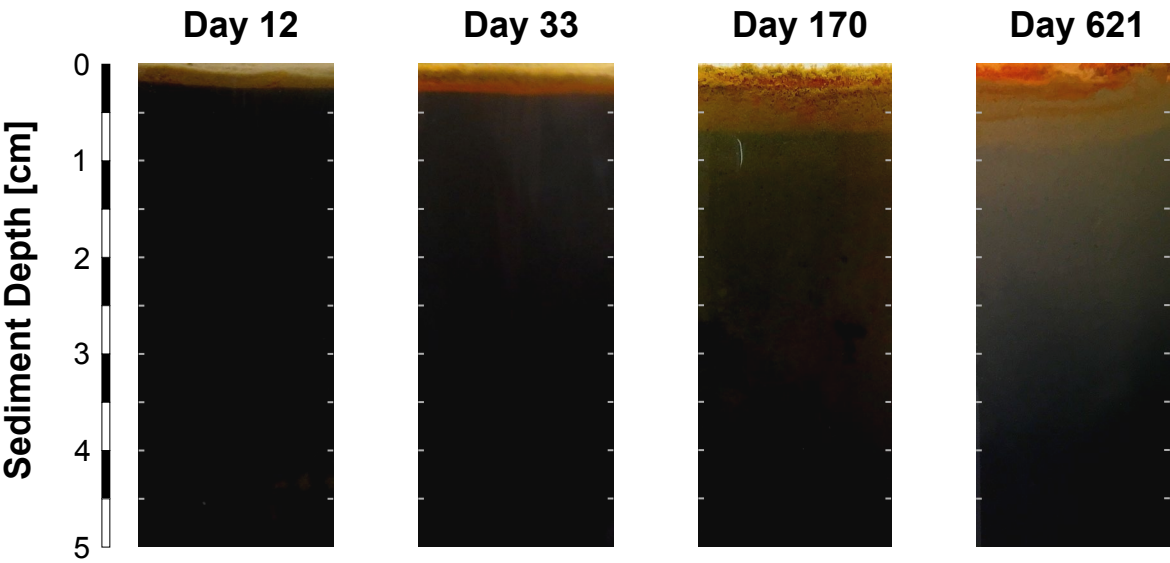


Figure S11. Time-series of Core Photographs. The scale bar intervals denote a distance of 0.5 cm.

S1.9. Time-series of Iron Speciation

Table S5. Iron speciation

	Depth (cm)	Fe oxides ($\mu\text{mol g}^{-1}$)	Fe (II) ($\mu\text{mol g}^{-1}$)	AVS ($\mu\text{mol g}^{-1}$)
Day 5				
	0 - 0.5	53.15	139.46	4.00
	0.5 - 1	15.37	166.25	10.75
	1 - 1.5	1.99	171.66	17.38
	1.5 - 2	3.85	169.46	22.59
	2 - 2.5	0.20	170.76	22.20
	2.5 - 3	1.22	168.81	24.05
	3 - 3.5	3.13	173.41	23.56
	3.5 - 4	1.05	176.38	24.57
	4 - 4.5	1.72	177.42	26.23
	4.5 - 5	1.48	172.61	25.03
Day 12				
	0 - 0.5	81.55	120.62	1.97
	0.5 - 1	16.58	151.39	12.16
	1 - 1.5	2.87	157.71	18.41
	1.5 - 2	2.58	164.69	20.10
	2 - 2.5	2.71	167.03	23.57
	2.5 - 3	2.71	175.84	23.04
	3 - 3.5	1.27	164.29	25.17
	3.5 - 4	1.35	174.46	24.27
	4 - 4.5	3.54	175.73	25.35
	4.5 - 5	2.45	177.38	25.31
Day 18				
	0 - 0.5	97.02	122.42	1.71
	0.5 - 1	17.45	145.63	9.16
	1 - 1.5	4.40	159.84	12.64
	1.5 - 2	1.53	168.80	20.84
	2 - 2.5	2.47	165.99	20.93
	2.5 - 3	1.72	174.74	24.62
	3 - 3.5	1.12	175.78	24.85
	3.5 - 4	3.60	177.05	24.72
	4 - 4.5	1.41	173.60	24.42
	4.5 - 5	2.12	173.78	25.60

Table S5. Iron speciation (continued)

Depth (cm)	Fe oxides ($\mu\text{mol g}^{-1}$)	Fe (II) ($\mu\text{mol g}^{-1}$)	AVS ($\mu\text{mol g}^{-1}$)
Day 26			
0 - 0.5	151.20	112.78	3.77
0.5 - 1	21.23	144.56	7.75
1 - 1.5	6.64	150.41	9.44
1.5 - 2	4.02	153.04	8.38
2 - 2.5	3.61	156.03	8.25
2.5 - 3	2.13	173.24	17.94
3 - 3.5	1.75	171.95	19.41
3.5 - 4	2.46	176.05	25.52
4 - 4.5	2.39	175.24	25.37
4.5 - 5	2.32	175.17	25.57
Day 33			
0 - 0.5	152.78	114.80	2.52
0.5 - 1	62.41	133.31	7.05
1 - 1.5	5.26	144.72	9.12
1.5 - 2	3.99	147.88	9.53
2 - 2.5	1.86	157.70	15.90
2.5 - 3	2.54	175.91	16.93
3 - 3.5	0.31	174.56	21.32
3.5 - 4	0.64	175.51	22.66
4 - 4.5	1.10	175.19	22.69
4.5 - 5	0.39	175.47	23.48
Day 40			
0 - 0.5	196.86	89.40	4.50
0.5 - 1	24.70	142.89	5.08
1 - 1.5	7.47	153.02	9.91
1.5 - 2.5	10.24	143.50	8.93
2.5 - 3	2.29	162.54	10.45
3 - 3.5	7.95	166.50	16.30
3.5 - 4.5	7.41	162.06	21.35
4.5 - 5	5.36	183.41	23.52

Table S5. Iron speciation (continued)

Depth (cm)	Fe oxides ($\mu\text{mol g}^{-1}$)	Fe (II) ($\mu\text{mol g}^{-1}$)	AVS ($\mu\text{mol g}^{-1}$)
Day 207			
0 - 0.5	303.25	36.88	2.42
0.5 - 1.5	29.60	117.44	3.93
1.5 - 2.5	3.43	142.02	5.36
2.5 - 3.5	3.33	148.26	14.89
3.5 - 4.5	1.71	174.95	22.33
4.5 - 5	2.97	189.49	23.64
Day 621			
0 - 0.5	484.78	7.61	0.27
0.5 - 1	98.60	47.59	0.94
1 - 1.5	17.50	89.26	2.09
1.5 - 2	14.42	114.36	3.84
2 - 2.5	12.73	145.52	6.80
2.5 - 3	6.89	158.41	11.49
3 - 3.5	3.01	161.37	18.16
3.5 - 4	1.22	166.28	22.44
4 - 4.5	0.95	169.97	23.21
4.5 - 5	1.34	170.89	23.53
Control			
0 - 0.5	2.62	190.82	37.52
0.5 - 1	1.70	187.20	31.76
1 - 1.5	1.87	182.64	28.26
1.5 - 2	2.13	178.94	25.87
2 - 3	2.42	174.36	27.01
3 - 4	3.92	173.78	31.11
4 - 5	3.96	176.56	31.37

S1.10. Time-series of Phosphorus Speciation

Table S6. Phosphorus speciation

Depth (cm)			Exchangeable P ($\mu\text{mol g}^{-1}$)	CDB-P ($\mu\text{mol g}^{-1}$)	Authigenic P ($\mu\text{mol g}^{-1}$)	Detrital P ($\mu\text{mol g}^{-1}$)	Organic P ($\mu\text{mol g}^{-1}$)
Day 5							
0	-	0.5	0.88	5.73	4.82	5.22	N/A
0.5	-	1	0.44	5.49	6.11	6.03	N/A
1	-	1.5	0.34	4.67	5.87	6.29	N/A
1.5	-	2	0.39	4.76	5.86	5.81	N/A
2	-	2.5	0.48	4.75	5.33	6.06	N/A
2.5	-	3	0.44	4.75	5.50	5.56	N/A
3	-	3.5	0.47	4.60	5.39	5.55	N/A
3.5	-	4	0.48	4.34	5.26	4.78	N/A
4	-	4.5	0.43	4.73	5.00	5.69	N/A
4.5	-	5	0.50	3.71	5.00	5.85	N/A
Day 12							
0	-	0.5	0.44	6.21	6.30	4.71	N/A
0.5	-	1	0.26	4.34	5.55	4.99	N/A
1	-	1.5	0.12	3.09	4.35	4.46	N/A
1.5	-	2	0.15	3.69	4.43	4.28	N/A
2	-	2.5	0.29	4.27	5.87	5.22	N/A
2.5	-	3	0.30	4.68	5.72	5.39	N/A
3	-	3.5	0.36	4.43	6.04	5.56	N/A
3.5	-	4	0.44	4.15	5.93	5.09	N/A
4	-	4.5	0.46	4.27	4.95	5.47	N/A
4.5	-	5	0.55	4.19	4.96	5.44	N/A
Day 18							
0	-	0.5	0.40	5.86	6.38	5.30	N/A
0.5	-	1	0.16	4.20	5.41	7.01	N/A
1	-	1.5	0.20	4.52	5.65	6.13	N/A
1.5	-	2	0.37	4.39	5.73	6.13	N/A
2	-	2.5	0.20	4.24	4.57	6.58	N/A
2.5	-	3	0.41	4.29	4.78	5.42	N/A
3	-	3.5	0.34	4.70	5.26	6.86	N/A
3.5	-	4	0.48	4.07	4.41	6.32	N/A
4	-	4.5	0.62	3.89	4.39	5.41	N/A
4.5	-	5	0.47	4.16	5.95	6.06	N/A

Table S6. Phosphorus speciation (continued)

Depth (cm)			Exchangeable P ($\mu\text{mol g}^{-1}$)	CDB-P ($\mu\text{mol g}^{-1}$)	Authigenic P ($\mu\text{mol g}^{-1}$)	Detrital P ($\mu\text{mol g}^{-1}$)	Organic P ($\mu\text{mol g}^{-1}$)
Day 26							
0	-	0.5	1.50	6.63	5.50	6.38	5.14
0.5	-	1	0.60	6.91	5.31	6.44	5.29
1	-	1.5	0.56	7.18	5.38	6.35	5.22
1.5	-	2	0.55	6.97	4.76	5.81	4.84
2	-	2.5	0.81	6.31	4.49	5.49	4.23
2.5	-	3	0.76	7.30	5.35	6.33	5.16
3	-	3.5	0.89	6.91	5.76	6.05	4.94
3.5	-	4	1.02	7.19	5.58	5.60	4.83
4	-	4.5	0.93	7.03	5.73	5.86	4.94
4.5	-	5	1.20	6.84	5.63	6.15	5.14
Day 33							
0	-	0.5	0.52	12.10	5.53	6.56	5.50
0.5	-	1	0.53	9.92	5.32	6.38	5.23
1	-	1.5	0.43	6.78	5.03	6.57	5.31
1.5	-	2	0.46	5.99	5.66	6.40	5.66
2	-	2.5	0.57	6.91	5.66	5.91	5.16
2.5	-	3	0.48	7.64	5.36	6.49	4.88
3	-	3.5	0.54	7.95	5.79	5.90	5.13
3.5	-	4	0.67	7.57	6.05	6.04	5.09
4	-	4.5	0.86	7.47	5.87	6.03	5.14
4.5	-	5	0.69	3.62	5.78	6.25	5.21
Day 40							
0	-	0.5	0.62	18.06	5.81	6.53	5.24
0.5	-	1	0.40	8.42	5.68	5.96	5.37
1	-	1.5	0.71	7.04	5.99	5.96	5.26
1.5	-	2.5	0.50	7.41	5.77	6.15	5.15
2.5	-	3	0.56	7.95	5.75	5.79	5.39
3	-	3.5	0.50	7.31	5.53	6.01	5.12
3.5	-	4.5	0.51	7.69	5.55	6.21	5.26
4.5	-	5	0.73	7.69	5.66	5.86	4.95

Table S6. Phosphorus speciation (continued)

Depth (cm)			Exchangeable P ($\mu\text{mol g}^{-1}$)	CDB-P ($\mu\text{mol g}^{-1}$)	Authigenic P ($\mu\text{mol g}^{-1}$)	Detrital P ($\mu\text{mol g}^{-1}$)	Organic P ($\mu\text{mol g}^{-1}$)
Day 207							
0	-	0.5	0.45	21.03	5.14	5.52	5.18
0.5	-	1.5	0.52	9.85	5.40	6.18	5.40
1.5	-	2.5	0.51	6.32	5.69	6.29	5.03
2.5	-	3.5	0.87	6.41	5.96	6.08	5.01
3.5	-	4.5	0.66	6.61	5.00	5.13	4.12
4.5	-	5	0.89	6.80	5.50	5.89	4.85
Day 621							
0	-	0.5	0.79	13.24	4.78	6.04	3.97
0.5	-	1	1.39	13.58	3.96	7.28	4.28
1	-	1.5	0.56	3.30	4.25	7.27	4.46
1.5	-	2	0.66	3.75	4.62	6.77	4.16
2	-	2.5	0.37	4.78	4.41	6.72	4.12
2.5	-	3	0.39	4.50	4.79	6.85	4.26
3	-	3.5	0.51	4.41	4.96	5.94	3.73
3.5	-	4	0.42	4.68	4.68	7.33	4.24
4	-	4.5	0.31	4.00	3.72	7.17	4.19
4.5	-	5	0.53	5.53	5.25	6.18	4.12
Control							
0	-	0.5	0.61	4.25	4.90	6.50	3.98
0.5	-	1	0.84	4.28	4.76	6.49	4.09
1	-	1.5	0.96	4.81	5.12	6.53	3.55
1.5	-	2	0.68	5.52	4.68	6.72	4.34
2	-	3	0.84	4.41	5.88	5.25	4.17
3	-	4	0.41	5.25	5.56	6.17	4.15
4	-	5	0.56	5.39	4.71	6.67	4.35

References

1. Boudreau, B. P. 1997. Diagenetic models and their implementation. Springer Berlin
2. Berner, R. A. 1980. Early diagenesis: a theoretical approach. Princeton University Press.
3. Burton, E. D., R. T. Bush, and L. A. Sullivan. 2006. Fractionation and extractability of sulfur, iron and trace elements in sulfidic sediments. *Chemosphere* **64**: 1421-1428.
4. Burton, E. D., L. A. Sullivan, R. T. Bush, S. G. Johnston, and A.F. Keene. 2008. A simple and inexpensive chromium-reducible sulfur method for acid-sulfate soils. *Applied Geochemistry* **23**: 2759-2766.
5. Claff, S. R., L. A. Sullivan, E. D. Burton, and R. T. Bush. 2010. A sequential extraction procedure for acid sulfate soils: partitioning of iron. *Geoderma* **155**: 224-230.
6. Fofonoff, N. P., and R. Millard Jr. 1983. Algorithms for the computation of fundamental properties of seawater.
7. Hermans, M., W. Lenstra, S. Hidalgo-Martinez, N. A. van Helmond, R. Witbaard, F. Meysman, S. Gonzalez, and C. P. Slomp. 2019. Abundance and Biogeochemical Impact of Cable Bacteria in Baltic Sea Sediments. *Environmental science & technology* **53**: 7494-7503.
8. Poulton, S. W., and D. E. Canfield. 2005. Development of a sequential extraction procedure for iron: implications for iron partitioning in continentally derived particulates. *Chemical Geology* **214**: 209-221.
9. Rao, A. M., S. Y. Malkin, S. Hidalgo-Martinez, and F. J. Meysman. 2016. The impact of electrogenic sulfide oxidation on elemental cycling and solute fluxes in coastal sediment. *Geochimica et Cosmochimica Acta* **172**: 265-286.
10. Ruttenberg, K. C. 1992. Development of a sequential extraction method for different forms of phosphorus in marine sediments. *Limnology and oceanography* **37**: 1460-1482.
11. Soetaert, K., T. Petzoldt, and F. Meysman. 2010. *Marelac*: Tools for aquatic sciences. R package version.
12. Slomp, C. P., E. H. Epping, W. Helder, and W. V. Raaphorst. 1996. A key role for iron-bound phosphorus in authigenic apatite formation in North Atlantic continental platform sediments. *Journal of Marine Research* **54**: 1179-1205.